Ad Hoc Networks 178 (2025) 103966

Contents lists available at ScienceDirect

Ad Hoc Networks

journal homepage: www.elsevier.com/locate/adhoc

Multi-UAV path planning for connectivity-based sweep coverage

Survi Kumari [a], Seshan Srirangarajan [a,b,*]

[a] Department of Electrical Engineering, Indian Institute of Technology Delhi, New Delhi, 110016, Delhi, India
[b] Bharti School of Telecommunication Technology and Management, Indian Institute of Technology Delhi, New Delhi, 110016, Delhi, India

ARTICLE INFO

Keywords:
Surveillance networks
Unmanned aerial vehicle (UAV)
Area coverage
Connectivity
Path planning
Mixed-integer linear programming (MILP)

ABSTRACT

Quality of service in wireless surveillance networks relies on two key factors: area coverage and connectivity. In this work, we investigate the spatial coverage and connectivity of a wireless surveillance network comprising of unmanned aerial vehicles (UAVs) used for surveying an area of interest. In many such applications, the data collected by the UAVs must be relayed, perhaps through multiple hops, to the base station in real-time. The goal of the network, in such applications, is to improve area coverage of the network while ensuring the UAVs are connected to the base station/sink throughout their flight. To achieve this, we propose two mixed-integer linear programming (MILP)-based formulations to plan the path of a set of UAVs. In the first formulation, we maximize the area covered by the UAVs while ensuring that they maintain their connectivity to the base station. In the second formulation, we minimize the number of movements required by the UAVs to achieve a desired coverage level while maintaining connectivity to the base station. We present extensive performance evaluation of the proposed algorithms and their comparison with path-planning approaches that do not consider connectivity constraints. We explore some of the trade-offs involved in meeting the connectivity requirement.

1. Introduction

Unmanned aerial vehicles (UAVs) are, nowadays, considered among the most effective tools for monitoring and tracking applications [1–3]. A network of connected UAVs enables each UAV to gather, process, store, and relay data through other UAVs until it reaches a base station (also known as the sink). This also allows the data from the UAVs to be available at the base station in real-time. The two main challenges in such monitoring or surveillance networks is to achieve maximum area coverage and ensuring that each UAV is able to communicate with the base station at all times. A number of studies have considered a network of UAVs for surveillance applications while maintaining robust communication capability within the network [4–6]. These studies show that ensuring connectivity during coverage path planning problems is not straightforward. Thus, some studies assume connectivity without explicitly incorporating it in their formulations [1]. It is clear that ensuring connectivity and achieving optimal area coverage cannot be achieved simultaneously and a trade-off is involved. This trade-off between coverage and connectivity in multi-UAV surveillance networks stems from opposing requirements: maximizing coverage requires the UAVs to spread out and explore newer areas, while maintaining connectivity requires them to remain within communication range of one another or the base station. If UAVs spread out too far to maximize coverage, they risk disrupting the communication links. On the other hand, clustering to preserve connectivity limits the overall area that can be covered. Therefore, to ensure continuous communication connectivity during coverage path planning, it is necessary to formulate the mobility strategies carefully.

1.1. Related work

Coverage path planning (CPP) for UAVs involves generating trajectories that ensure complete area coverage, often under constraints such as energy, time, or communication. Depending on the mission objectives, CPP can be continuous, ensuring a persistent coverage over the area of interest, or periodic, revisiting areas at regular intervals. These problems are commonly formulated as optimization problems to systematically explore the trade-offs and satisfy operational requirements. Galan-Jimenez et al. [7] formulate 3D energy-aware mission planning (3DEE-UMP) as a mixed integer linear programming (MILP) problem. Their approach enables UAVs to operate at different altitudes to balance area coverage with energy consumption. They propose a genetic algorithm-based heuristic to ensure continuous coverage while minimizing battery depletion and recharging needs. While this model focuses on altitude-driven coverage efficiency, it assumes reliable connectivity for communication without explicitly modeling it.

* Corresponding author at: Department of Electrical Engineering, Indian Institute of Technology Delhi, New Delhi, 110016, Delhi, India.
E-mail addresses: Survi.Kumari@ee.iitd.ac.in (S. Kumari), seshan@ee.iitd.ac.in (S. Srirangarajan).

https://doi.org/10.1016/j.adhoc.2025.103966
Received 9 December 2024; Received in revised form 20 May 2025; Accepted 4 July 2025
Available online 19 July 2025
1570-8705/

Table 1
Multi-UAV mobility strategies for coverage path planning (CPP) and connectivity (Conn.)

Reference	CPP	Conn.	Mobility strategy
Danoy et al. [4]	✓	✓	Pheromone and clustering-based
Messous et al. [5]	✓	✓	Virtual force-based
Yanmaz [6]	✓	✓	Virtual force-based
Rosalie et al. [9]	✓	✓	Pheromone and force-based
Li et al. [10]	✓	✗	Optimization and heuristic-based
Liu et al. [11]	✓	✗	Heuristic-based
Chen et al. [12]	✓	✗	MILP and clustering-based
Lamine et al. [13]	✓	✓	Integer linear prog. (ILP)-based
Kumari et al. [14]	✓	✗	MILP-based
Our work	✓	✓	MILP-based

Zhou et al. [8] study the handover and coverage performance in 3D UAV cellular networks, where UAVs act as aerial base stations (UAV-BSs). Using stochastic geometry, they model multi-altitude deployments and analyze how mobility, link state transitions (LoS/NLoS), and user association strategies affect network performance. Their model assumes continuous coverage but does not account for specific UAV paths or mission planning. [8] aims to maintain UAV connectivity while taking a theoretical and network-centric view of the solution methodology.

Given the diverse applications requiring UAV collaboration, multi-UAV path planning is commonly encountered in tasks such as target search, internet of things (IoT)-based data collection, surveillance, and monitoring. Maintaining connectivity between the UAVs, ground base stations, and other network entities is crucial for ensuring reliable communication and enabling seamless data collection and transmission. Since in this work, we focus on UAV path planning for connectivity-based sweep coverage, we restrict the remainder of this section to reviewing studies that specifically address connectivity-aware path planning.

In [6], a force-based probabilistic mobility model is presented for UAVs. They explored the trade-off between area coverage and maintaining connectivity of a set of UAVs with the base station. However, due to the probabilistic nature of the algorithm, disconnections from the sink can occur in some instances. The authors in [9] presented a method that combines ant colony optimization (ACO) with a chaotic dynamical system and the Boids flocking model for maximizing area coverage while preserving connectivity within a UAV swarm.

In [10], Li et al. presented a sweep coverage method to efficiently patrol a set of targets. They prioritize the targets by assigning different weights to them and each UAV maximizes the sum of the weights of the covered targets. In [11], Liu et al. addressed sweep coverage with return time constraints. They presented two heuristic methods to determine the minimum number of mobile sensors that are required to cover the targets so as to be able to return to the base station and deliver the collected data within a predefined time window. In [12], the authors carried out coverage path planning of a team of heterogeneous UAVs on a given number of regions. They presented a mixed-integer linear programming (MILP)-based flying strategy for UAVs and employed a clustering-based approach to classify regions into clusters. In [10–12], the UAVs/mobile sensors are expected to return to the base station with the recorded data but connectivity requirements during the flight has not been considered.

Lamine et al. [13] developed two routing models to minimize the transportation cost for a set of UAVs to monitor an area without exceeding the individual flight time limit for each UAV. They also ensure connectivity of each UAV to the base station during flight while assuming that the data can be relayed to the base station via multiple hops (i.e., UAVs). The various mobility strategies used to address the area coverage and connectivity in a network are summarized in Table 1.

The authors in [15] have investigated the path planning challenge for a UAV mesh network tasked with collecting data from ground-based IoT devices while aiming to minimize the maximum age of information (AoI) [16–18]. With AoI being determined by the data delivery time to the backhaul/base station, ILP problem formulation is used to find the optimal path and a mesh topology of UAVs is used for minimizing the maximum AoI.

Some more recent works on coverage path planning of multi-UAV systems with connectivity constraints consider cellular-connected UAVs. In a cellular-connected UAV network, the UAVs are equipped with cellular communication capabilities to establish connectivity with ground-based cellular networks. The system model in such networks is different from the one used in this work. Instead of one, there are several ground stations (or base stations) available for connectivity and each UAV needs to complete its mission of flying from the start point to the destination while avoiding collision with other UAVs. Moreover, inter-UAV communication is not necessary. Among the methods used for trajectory design in cellular-connected UAVs, deep reinforcement learning (DRL)-based solutions [19–22] have gained significant popularity. These methods are capable of dealing with complex and dynamic environments (real-time path planning solutions), however, it is worth noting that RL-based methods may not always yield the optimal path. Other challenges include the need for extensive training data and instability during training. On the other hand, MILP-based algorithms offer advantages in UAV path planning due to their optimality guarantees. They can incorporate real-world constraints effectively and produce consistent results.

In a more recent work [23], coverage and connectivity trade-off is studied as a multi-objective optimization problem. The authors presented a multi-objective evolutionary algorithm (MOEA) based on NSGA-II and NSGA-III, to optimize UAV trajectories by optimizing for continuous connectivity through direct or multi-hop links. The presented approach demonstrates superior flexibility compared to weighted-sum optimization and reinforcement learning-based methods, offering Pareto-optimal solutions. However, they are able to achieve only periodic or discontinuous connectivity which is a drawback for emergency/post-disaster surveillance applications.

1.2. Our contributions

The main contribution of this work is the novel approach of incorporating the connectivity requirement of the UAVs to the base station in a multi-agent wireless surveillance network and formulating it as an MILP. This work can be considered as a novel extension of our previous work [14], where the path of a set of mobile sensor nodes is designed to achieve optimal coverage in a mixed wireless sensor network. The goal here is to enhance the proposed system model and its applicability in real-world scenarios by including connectivity requirements. To achieve the above mentioned objective, we develop two MILP-based formulations for planning the path of a set of UAVs for achieving effective area coverage and ensuring continuous connectivity to the base station. The first formulation is aimed at maximizing the area coverage, while the second formulation is aimed at minimizing the number of movements required by the UAVs to achieve a desired level of area coverage. Both the formulations ensure connectivity of each UAV to the base station, through multiple inter-UAV links, during the coverage path planning of the multi-UAV system. This is achieved by introducing two key constraints: (i) at least one UAV must always remain within the communication range of the base station, and (ii) UAVs that are not directly connected to the base station must maintain communication link(s) with other UAVs that are within the communication range of the base station. Additionally, for a more resource-efficient and robust network, we incorporate a constraint to prevent collision among UAVs. The key contributions of our work are listed below:

- An MILP-based formulation that plans the path of a set of UAVs for maximizing the area coverage within a given number of time steps while maintaining connectivity of each UAV to the sink either directly or through other UAVs acting as relays.
- An MILP-based formulation for planning the path of a set of UAVs while minimizing the number of movements required by the UAVs to achieve a desired area coverage level, along with ensuring multi-hop connectivity of each UAV to the sink.

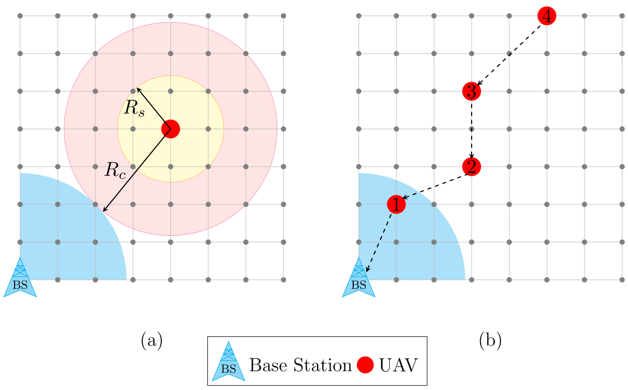

Fig. 1. A typical system model with a base station located at the bottom-left corner. The blue-shaded region around the base station indicates the communication range of the base station. (a) Two concentric circles around the UAV indicate its sensing and communication regions with $R_s = \sqrt{2}$ and $R_c = 2R_s$, (b) Connectivity path between four UAVs and the base station.

1.3. Outline

The remainder of the paper is organized as follows. The system model and its characteristics are described in Section 2. In Section 3, the proposed MILP-based path planning strategies are presented. In Section 4, performance evaluation of the proposed algorithms is presented. Finally, the paper is concluded in Section 5. Please note that the terms base station and sink are used interchangeably in this article.

2. System model

Consider the coverage area of interest to be a rectangular region of size $X \times Y$ and discretized into XY uniformly spaced grid points. A set of N UAVs (or mobile nodes) are to be used to monitor/sense this area and relay the sensed data in real-time to the base station via multi-hop connectivity through other UAVs. The goal is to plan the path of these cooperating UAVs such that all the grid points within the area of interest are covered (at least once) by at least one UAV (1-coverage). In addition, all the UAVs are required to maintain connectivity to the base station either directly or through other UAVs throughout their path to ensure that the data can be relayed to the base station in real-time.

A binary disk model for the communication channel is assumed. In this model, the communication is assumed to be perfect as long as a UAV is within the communication range of another UAV or the base station. Each UAV is assumed to be equipped with a communication transceiver (with omnidirectional antenna) with a range R_c and sensor(s) with a sensing range of R_s. Thus, a UAV can sense/cover all the grid points which are within a distance R_s from it. Similarly, a UAV can communicate with other UAVs (and possibly the base station) which are within a distance R_c from it. This allows for multi-hop connectivity of the UAVs to the base station. The UAVs are assumed to fly at a fixed altitude. In one time step, we assume the UAVs can move to any grid point within R_c distance from its current location. The path of UAVs is computed offline and is subject to revision only in the event of significant changes to the physical structure of the area of interest.

Fig. 1 illustrates the system model and the connectivity requirements. In Fig. 1(b), we show that UAV-1 has a single-hop (direct) connectivity with the base station, while the other three UAVs have multi-hop connectivity to the base station. The key parameters of the proposed system model are listed in Table 2. It is important to note that we use linear indices to reference the grid points in all our formulations.

Table 2
List of system parameters, decision variables, and their notations.

Symbol	Definition
s	Base station (or sink) location
$\mathcal{G}_{\bar{s}}$	Set of all the grid points in the area of interest (Note: $\bar{s}$ indicates that the sink location is excluded from this set)
C_s	Set of grid points within the communication range of the sink location s
C_i	Set of grid points within the communication range of the grid point i
S_i	Set of grid points within the sensing range of the grid point i
N	Number of UAVs (or mobile nodes)
$K_{\max}$	Maximum number of time-steps
$C_{\max}$	Total number of grid points to be covered (Note that, $C_{\max} = \lvert\mathcal{G}_{\bar{s}}\rvert$, the cardinality of $\mathcal{G}_{\bar{s}}$)
cr	Area coverage ratio: ratio of the number of grid points covered at least once at any time-step and $C_{\max}$ $(0 \le cr \le 1)$
$z_{i,n}^k$	Binary variable; $z_{i,n}^k = 1$ if the nth UAV is located at grid point i at the kth time-step, otherwise $z_{i,n}^k = 0$.
$c_{i,n}^k$	Continuous variable; $c_{i,n}^k = 1$ if the grid point i is covered by the nth UAV at the kth time-step, otherwise $c_{i,n}^k = 0$.
c_i	Continuous variable; $c_i = 1$ if the grid point i is covered by any UAV at any time-step, otherwise $c_i = 0$.

3. Path planning strategies

In this section, we describe the two proposed MILP-based path planning strategies for a set of UAVs to achieve efficient sweep coverage of the area of interest while being able to send the sensed data in real-time to the base station via multi-hop connectivity through other UAVs. Let s denote the base station location and binary position variable $z_{i,n}^k$ indicate location of the nth UAV. Also, let $c_{i,n}^k$ and c_i be the coverage variables. These parameters/variables are defined in Table 2.

3.1. Coverage maximization (max-Cov)

In this formulation, referred to as max-Cov, we plan the paths of the UAVs so as to maximize the area coverage, in terms of the number of grid points covered, in a given number of time-steps, and while maintaining multi-hop connectivity of each UAV to the base station. Below, we provide the mathematical expressions of the proposed MILP formulation, followed by a detailed description of the objective function and the constraints.

$$\max \sum_{i \in \mathcal{G}_{\bar{s}}} c_i \tag{1}$$

$$\text{s.t.} \sum_{i \in \mathcal{G}_{\bar{s}}} z_{i,n}^k = 1\ ; \quad n = 1, \ldots, N; k = 1, \ldots, K_{\max} \tag{2}$$

$$\sum_{n=1}^{N} z_{i,n}^k \le 1\ ; \quad \forall i \in \mathcal{G}_{\bar{s}}; k = 1, \ldots, K_{\max} \tag{3}$$

$$\sum_{n=1}^{N} \sum_{p \in C_s} z_{p,n}^k \ge 1\ ; \quad k = 1, \ldots, K_{\max} \tag{4}$$

$$z_{i,n}^k \le \sum_{p \in C_i} z_{p,(n-1)}^k\ ;\ \forall i \in \mathcal{G}_{\bar{s}}; n = 2, \ldots, N; k = 1, \ldots, K_{\max} \tag{5}$$

$$z_{i,n}^{k+1} \le \sum_{p \in C_i} z_{p,n}^k\ ;\ \forall i \in \mathcal{G}_{\bar{s}}; n = 1, \ldots, N; k = 1, \ldots, (K_{\max-1}) \tag{6}$$

$$c_{i,n}^k = \sum_{p \in S_i} z_{p,n}^k\ ;\ \forall i \in \mathcal{G}_{\bar{s}}; n = 1, \ldots, N; k = 1, \ldots, K_{\max} \tag{7}$$

$$c_i \ge c_{i,n}^k\ ; \quad \forall i \in \mathcal{G}_{\bar{s}}; n = 1, \ldots, N; k = 1, \ldots, K_{\max} \tag{8}$$

$$c_i \le \sum_{k=1}^{K_{\max}} \sum_{n=1}^{N} c_{i,n}^k\ ; \quad \forall i \in \mathcal{G}_{\bar{s}} \tag{9}$$

$$0 \le c_i, c_{i,n}^k \le 1\ ;\ \forall i \in \mathcal{G}_{\bar{s}}; n = 1, \ldots, N; k = 1, \ldots, K_{\max} \tag{10}$$

Objective function: The coverage variable c_i indicates whether the grid point i has been sensed/covered by any UAV or not. Our purpose is to maximize the number of grid points that are covered. The objective function thus involves a sum of the coverage variable values for each grid point.

Position constraint: In order to ensure that each UAV is at only one grid point at a time-step, the position variable for each UAV over all the grid points must sum up exactly to 1. In simpler terms, it guarantees that a UAV cannot occupy multiple grid points simultaneously. This can be represented mathematically as in (2).

Collision avoidance constraint: During their paths each UAV must avoid collision with the other UAVs to prevent any physical damage. This can be achieved if a grid point can be visited by at most one UAV in a given time-step. This condition is expressed mathematically in (3).

The robustness of any wireless surveillance network is measured by its ability to deliver the data to the base station in real-time, which depends on the network connectivity. Given the limited communication range of UAVs, ensuring continuous connectivity between UAVs and the base station is imperative. Our strategy to ensure multi-hop connectivity is illustrated in Fig. 1(b).

Sink connectivity constraint: In order to ensure continuous connectivity to the base station, at least one UAV must be within its communication range at each time step. Thus, sum of the position variables of all UAVs for the grid points within the communication range of the base station should be greater than or equal to 1 at each time-step. This also implies that more than one UAV can be directly connected to the base station at any time-step. This constraint is represented mathematically in (4).

Inter-UAV connectivity constraint: We assume that the UAVs can maintain connectivity with the base station via multi-hop connectivity with the other UAVs acting as relays. This can be achieved if each UAV remains within the communication range of at least one UAV at each time-step. If the nth UAV is at grid point i, then one or more UAVs must be at grid points within its communication range in order to ensure inter-UAV communication. This constraint is represented as (5).

Mobility constraint: The movement range of UAVs is assumed to be equal to their communication range and each UAV can move only once at each time-step. If a UAV is at grid point i at a time-step, then it must have been at one of the grid points within its communication range in the previous time-step. This is expressed as constraint (6).

Coverage constraints: To define coverage constraints, we map the coverage achieved by each UAV onto a global coverage variable c_i. A variable $c_{i,n}^k$ is defined to account for grid points covered by each UAV individually at each time-step. Constraint (7) is an equality constraint that ensures a grid point i is considered as covered, by the nth UAV at the kth time-step, if the grid point i is within the sensing range of the nth UAV.

Constraints (8) and (9) are used to map the individual coverage of UAVs to the global coverage of the network area. It is worth noting that a grid point could be covered more than once primarily due to two reasons: (i) traveling/movement and sensing ranges of UAVs are limited due to which multiple UAVs may visit a grid point across different time-steps to reach uncovered grid points, and (ii) UAVs need to be within the communication range of at least one other UAV in order to maintain network connectivity. Thus, (8) ensures that a grid point that has been covered in any time-step by any UAV is considered to be covered throughout the rest of the algorithm. Constraint (9) sets c_i to 0 if the grid point i has not been covered by any UAV in any time-step.

Constraint (10) defines the limits for the continuous variables c_i and $c_{i,n}^k$. This ensures that the value of these variables does not exceed 1, even if the corresponding grid points are covered multiple times.

3.2. Movement minimization (min-Mov)

In this formulation, referred to as min-Mov, we plan the paths of a set of UAVs by minimizing the total number of movements required by the UAVs to attain a desired coverage level, while maintaining multi-hop connectivity. The desired coverage level is defined by the area coverage ratio cr, where $0 \le cr \le 1$.

$$\min \sum_{k=1}^{K_{\max}} \sum_{\substack{n=1 \\ i\in\mathcal{G}_{\overline{S}}}}^{N} z_{i,n}^k \tag{11}$$

$$\text{s.t.} \sum_{i\in\mathcal{G}_{\overline{S}}} z_{i,n}^k \le 1 \ ; \ n = 1,\dots,N; k = 1,\dots,K_{\max} \tag{12}$$

$$\sum_{i\in\mathcal{G}_{\overline{S}}} c_i \ge cr \cdot C_{\max} \tag{13}$$

Constraints (3), (4), (5), (6), (7), (8), (9), (10)

The objective function in (11) minimizes the number of grid points visited by all the UAVs while achieving the desired coverage ratio. Note that visiting a grid point and covering a grid point have different implications. The number of grid points visited by the UAVs represents the number of movements by the UAVs. Position constraint (12) is similar to the constraint in (2) except that it allows the possibility that after a certain number of time-steps, $z_{i,n}^k$ for each UAV is set to zero. The connectivity, mobility, and coverage constraints are the same as in the coverage maximization formulation. Constraint (13) ensures that the total coverage achieved by the UAVs must satisfy the desired coverage level.

It is to be noted that the area coverage strategy of the proposed algorithms is similar to our previous work [14] except for the limit on overlapping coverage. In this work, overlapping coverage has been leveraged to meet the multi-hop connectivity requirements. It is also to be noted that even though c_i and $c_{i,n}^k$ are defined as continuous variables in the range $[0,1]$, they will essentially behave as binary variables. This is because the constraints have been formulated in such a way that they can only take values 0 or 1. They have been defined as continuous variables to reduce the complexity of the integer linear programs (ILPs), as the complexity of ILPs is known to increase exponentially with the number of binary/integer variables [1].

4. Results and discussion

In this section, we present detailed performance analysis of the proposed connectivity-based path planning strategies for efficient area coverage. The area of interest is assumed to be obstacle-free and the coverage area is two-dimensional. The UAVs are assumed to move with a constant velocity at a fixed altitude. The base station is assumed to be placed at the center or at one of the corners of the rectangular area of interest. The algorithms were implemented in MATLAB R2020b and used the 12.10.0 version of the IBM ILOG CPLEX optimization software. The CPLEX parameter settings used include 'TimeLimit' of 18000 s, 'MIPGap' of 0, and branch and cut as the 'MIP Strategy Search'. The simulations were carried out on a workstation with Intel(R) Core(TM) i7-4770 CPU @ 3.40 GHz, 16 GB RAM, and running Microsoft Windows 10.

4.1. Coverage maximization performance

First, we present performance analysis of the proposed max-Cov path planning strategy based on maximizing the area coverage. The area coverage (%) or the percentage of covered grid points is computed as the ratio of the total number of grid points covered at least once (across all time-steps) and $C_{\max}$, i.e., $\frac{\left(\sum_{i\in\mathcal{G}_{\overline{S}}} c_i\right)}{C_{\max}} \times 100$, where c_i is the coverage variable at each grid point i with its value becoming 1 if a UAV covers it at any time-step. Once a grid point is marked as

Table 3
Area coverage and computation time using the coverage maximization (max-Cov) strategy ($K_{max} = 4$)

Grid size	No. of UAVs	Sink location	Area coverage (%)	Computation time (s)
5 × 5	2	Corner	100	0.193
6 × 6			100	0.169
7 × 7			72.92	1.038
8 × 8			55.56	1.060
5 × 5	2	Center	100	0.072
6 × 6			100	0.185
7 × 7			91.67	6.144
8 × 8			76.19	97.281
5 × 5	3	Corner	100	0.114
6 × 6			100	0.255
7 × 7			95.83	90. 645
8 × 8			87.30	132.087
5 × 5	3	Center	100	0.143
6 × 6			100	0.273
7 × 7			100	0.756
8 × 8			96.83	421.191

covered it remains so for one complete execution of the algorithm. C_{max} denotes the total number of grid points to be covered in the target area excluding the grid point where the sink is located.

In Table 3, it is seen that the UAVs are able to cover a much smaller area when the base station is at a corner location than at the center within a fixed number of time-steps. The is due to the fact that when the base station is placed at a corner location, the area of its communication region is one-fourth of that when it is placed at the center. In Fig. 2, we compare the area coverage performance of the proposed max-Cov path planning strategy with connectivity requirements and the strategy in [14] (with mobile nodes' overlap factor, $\hat{m}_o = 3$) which does not consider any connectivity constraints. In the absence of connectivity constraints, the UAVs using the method in [14] can move independently within their mobility range, allowing them to cover a larger area. However, in the proposed max-Cov method, UAVs are required to stay within communication range of one another and maintain connectivity to the base station, which limits how far they can spread out. As a result, while the proposed strategy ensures continuous network connectivity, it is achieved at the cost of reduced area coverage. This trade-off can be clearly observed in Fig. 2. It is seen that the area coverage decreases significantly when the connectivity constraints are included as well as when the base station is placed at a corner location.

In Fig. 2, we also present the overlap coverage value for each of the strategies. The overlap coverage value is computed by subtracting the effective coverage from the total number of times (all) the grid points are covered over all time-steps. The overlap coverage value reported when the base station is at a corner is the average of the values obtained when the base station is at each of the four corners. These results indicate the trade-off between achieving efficient area coverage and meeting the connectivity requirements. The continuous connectivity requirement of UAVs to the base station can significantly reduce the area coverage performance while increasing the overlap coverage value. In Fig. 3, we show the evolution of the area coverage as the maximum number of time-steps are increased for different number of UAVs. It is seen that the area coverage increases with the number of allowed time-steps and eventually achieves full (100%) area coverage. Also, the rate of area coverage improves with the number of UAVs.

4.2. Movement minimization performance

In Table 4, we compare performance of the proposed movement minimization-based min-Mov path planning strategy for different values of R_s and R_c. We consider a 12×12 grid size with three UAVs and a desired coverage level given by $cr = 0.95$. For a given R_s, the total

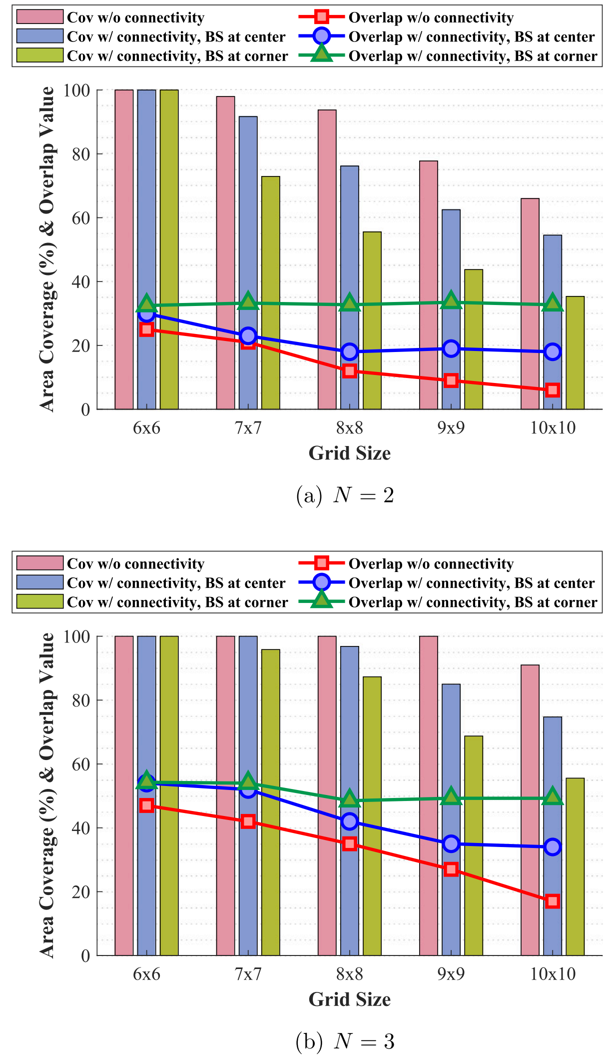

(a) $N = 2$

(b) $N = 3$

Fig. 2. Area coverage and average overlapping coverage for path planning with and without connectivity constraints for different grid sizes and number of UAVs. $R_s = \sqrt{2}$, $R_c = 2R_s$, and $K_{max} = 4$.

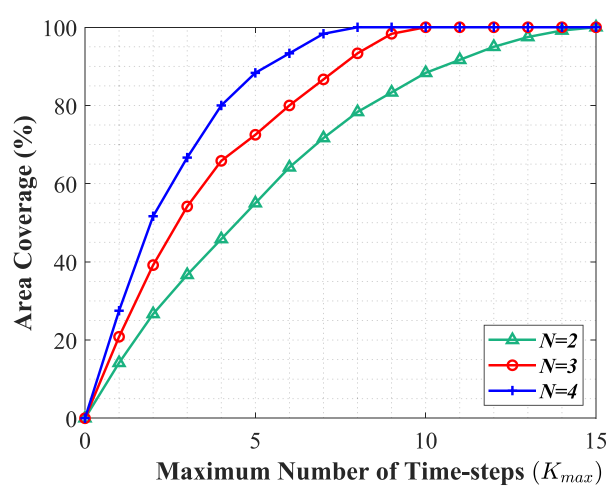

Fig. 3. Area coverage as a function of the maximum number of time-steps (K_{max}) with different number of UAVs. Grid size is 11×11, $R_s = \sqrt{2}$, $R_c = 2R_s$ and base station is at the center.

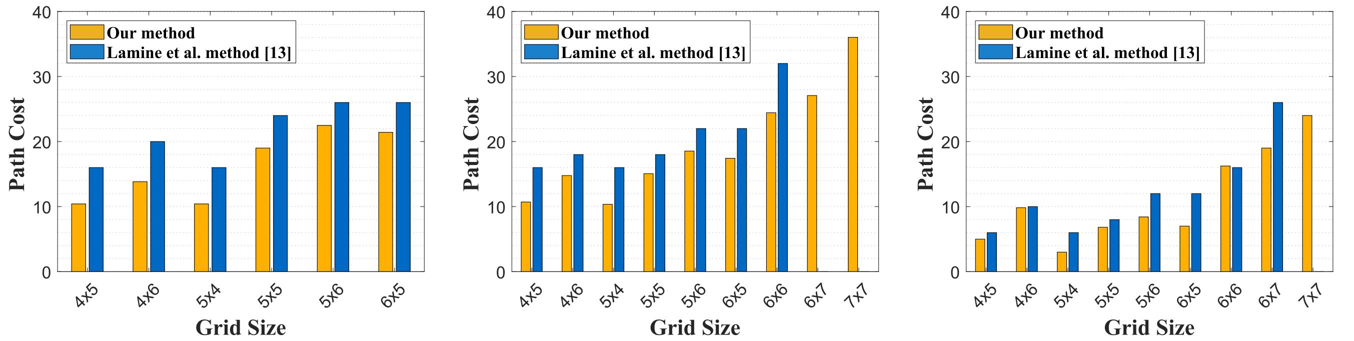

(a) $R_s = 1$ and $R_c = 2$ (b) $R_s = 1$ and $R_c = 3$ (c) $R_s = 2$ and $R_c = 2$

Fig. 4. Comparison of path cost for full (100%) coverage for different grid sizes, and different R_c and R_s values with two UAVs.

Table 4
Performance of movement minimization strategy with different sensing and communication ranges. Grid size is 12×12, $N = 3$, and $cr = 0.95$.

R_s	R_c	No. of movements
1	3	47
	4	37
	5	30
$\sqrt{2}$	3	28
	4	18
	5	16
2	3	27
	4	17
	5	15

number of movements required by the UAVs decreases as R_c increases. Similarly, for a given R_c, the number of movements decrease as R_s increases. As R_s and R_c increase, the UAVs are able to cover a larger area and travel farther at each time-step without losing connectivity, resulting in an improved optimal solution.

In Fig. 4, we show the cost of the paths obtained using the proposed min-Mov method and the method by Lamine et al. [13] with two UAVs, and for different grid sizes, and R_s and R_c values. The path planning is carried out so as to achieve full (100%) coverage and the sink is placed at the center of the area of interest in each case. For a fair comparison of the two methods, initial locations of UAVs are assumed to be the same as the sink location and the computation time limit is set to 3600 s as in [13]. The cost of a path is defined as the sum of the Euclidean distances between the grid points along the path. It is seen from Fig. 4 that the cost incurred for paths obtained using our proposed method are smaller than that using the method in [13] (Note that results for the Lamine et al. method are obtained from Table 4 in [13]). Only in the case with $R_s = 2$, $R_c = 2$, and 6×6 grid size, our proposed method results in a path with a slightly higher cost compared to [13]. This is due to the fact that our proposed method results in a path where one of the UAVs revisits the sink along its path. Additionally, with $R_s = 1$, $R_c = 3$, and $R_s = 2$, $R_c = 2$, when the grid size exceeds 6×6 and 6×7, respectively, the method proposed by Lamine et al. fails to generate a path within the computation time limit, whereas our proposed method is able to determine the optimal paths.

In Fig. 5, we show the paths of three UAVs obtained using the proposed movement minimization-based strategy with connectivity constraints. We consider a grid size of 11×11 with base station at the center, three UAVs, $R_s = \sqrt{2}$, $R_c = 2R_s$, $cr = 1$, and $K_{\max} = 10$. It is seen that the three UAVs are able to achieve full coverage in 27 movements and their paths are shown with different colored lines. At the first step, the third UAV (green color) is directly connected to the base station (green(1) → BS), whereas the second UAV (blue color) is two-hops from the base station (blue(1) → green(1) → BS), and the first UAV (red) is three-hops from the base station (red(1)→ blue(1) → green(1) → BS).

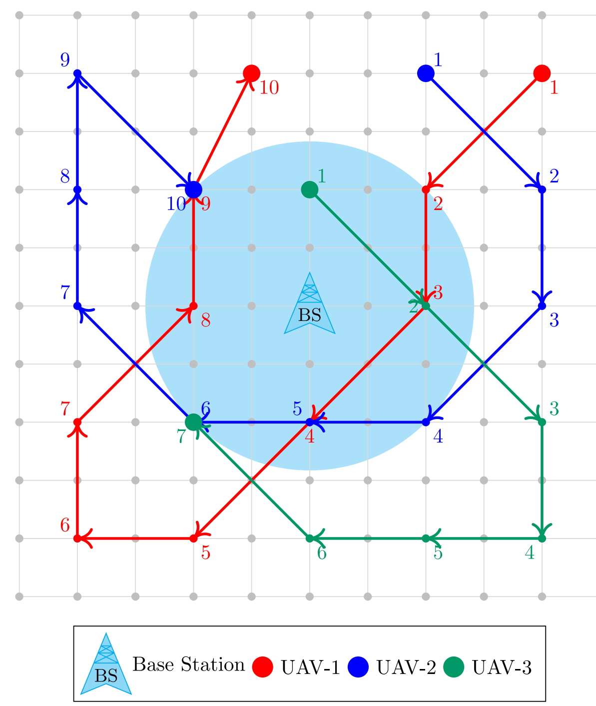

Fig. 5. Coverage paths obtained using the movement minimization strategy for a 11×11 grid size and three UAVs with connectivity to the base station.

Similarly, it can be seen that at each time step at least one of the UAVs is directly connected to the base station and other UAVs are connected to the base station through multiple hops. It is noted that the third UAV (green) stops after 7 movements as a result of constraint (12).

It is important to note that the two MILP-based formulations, max-Cov and min-Mov, proposed in this work operate independently based on their input parameters. Each solves the path planning problem using its own objective function and constraints. The input parameters include the number of UAVs, grid size, sink location, communication and sensing ranges (R_c and R_s), and the maximum number of time-steps ($K_{\max}$). For the movement minimization formulation, an additional parameter, cr, is also considered. Despite their differences, both formulations are designed to maintain network connectivity at every time-step. Each UAV remains connected to the base station, either directly or through other UAVs in a multi-hop manner.

Fig. 6 shows the evolution of the achieved coverage ratio (cr) with the total number of movements by the UAVs under connectivity constraints, for both the coverage maximization (max-Cov) and movement minimization (min-Mov) algorithms. The coverage maximization approach achieves a slightly higher initial coverage ratio, achieving over

Table 5
Comparison of the number of constraints and variables.

Method	No. of integer Variables	No. of continuous Variables	No. of Constraints
max-Cov	$NK_{\max}\lvert\mathcal{G}\rvert$	$(1+NK_{\max})\lvert\mathcal{G}\rvert$	$(1+4NK_{\max}-N)\lvert\mathcal{G}\rvert + (1+N)K_{\max}$
min-Mov	$NK_{\max}\lvert\mathcal{G}\rvert$	$(1+NK_{\max})\lvert\mathcal{G}\rvert$	$(1+4NK_{\max}-N)\lvert\mathcal{G}\rvert + (1+N)K_{\max} + 1$

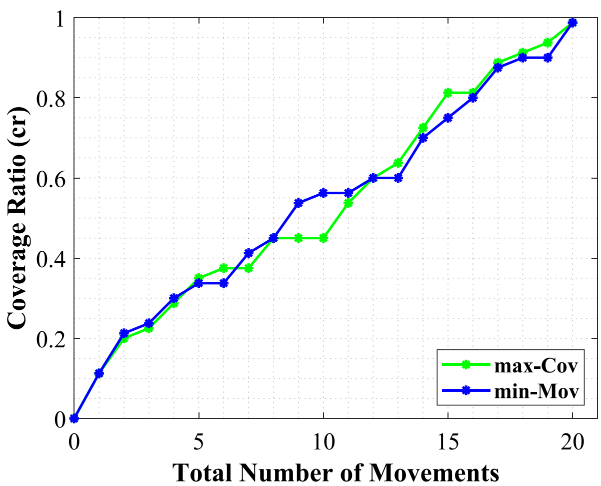

Fig. 6. Comparison of coverage ratio versus number of movements with two UAVs ($N = 2$) for a grid size of 9×9 with $R_s = \sqrt{2}$, $R_c = 2R_s$, and base station at the center.

80% area coverage with fewer movements. In contrast, the movement minimization method exhibits a relatively slower coverage progression, requiring a few more movements to reach the same coverage levels. However, it achieves this with reduced movement cost, making it more energy-efficient. Both the algorithms eventually converge to a coverage ratio of $cr = 0.9875$, but the trade-off between coverage improvement and movement efficiency is clearly observed. Importantly, both approaches successfully maintain connectivity to the base station at all time-steps, ensuring uninterrupted network communication during the entire mission. These results highlight the effectiveness of the coverage maximization method in time-critical scenarios, while the movement minimization algorithm is better suited for energy-constrained missions.

4.3. Computational complexity

We analyze the complexity of the proposed algorithms in terms of the number of continuous variables, number of integer variables, and the number of constraints. These are listed in Table 5. It is seen that these complexity measures increase linearly with the grid network size and the number of UAVs. Although the two path planning algorithms, coverage maximization (max-Cov) and movement minimization (min-Mov), differ only by one constraint, larger run-times are observed for movement minimization compared to coverage maximization. This is because the objective function of the movement minimization formulation involves integer/binary variables, and the complexity of ILP increases exponentially with integer/binary variables.

To further illustrate this, we compare the complexity of the proposed movement minimization method with the CPPC algorithm by Lamine et al. [13]. The comparison is based on the number of decision variables and constraints. Consider a setting with $N = 3$, $K_{\max} = 4$, and $\lvert\mathcal{G}\rvert = 30$.

(a) *Complexity analysis for the movement minimization algorithm*:
Number of variables (integer and continuous) $= NK_{\max}\lvert\mathcal{G}\rvert + (1+NK_{\max})\lvert\mathcal{G}\rvert$ $\quad$ ($=$ **750**)
Number of constraints $= (1+4NK_{\max}-N)\lvert\mathcal{G}\rvert + (1+N)K_{\max} + 1$ $\quad$ ($=$ **1397**)
The initial location constraints require N additional constraints, resulting in total number of constraints as **1400**

(b) *Complexity analysis for the CPPC algorithm* (Lamine *et al.* [13]):
Number of variables $= (\lvert\mathcal{G}\rvert + K_{\max})N\lvert\mathcal{G}\rvert$ $\quad$ ($=$ **3060**)
Number of constraints $= (2+N+N\lvert\mathcal{G}\rvert)K_{\max}\lvert\mathcal{G}\rvert + (1-N)\lvert\mathcal{G}\rvert^2 + (2+K_{\max})N$ $\quad$ ($=$ **9618**)

The CPPC algorithm [13] has 7 times more constraints and over 4 times more decision variables than the proposed formulation for the assumed parameter values. This significant difference in complexity highlights the computational efficiency of the proposed approach compared to [13], making it more scalable and practical for real-world applications.

5. Conclusion

We have proposed two MILP-based algorithms for planning the paths of a set of UAVs while ensuring continuous connectivity with the base station for sweep coverage. The first algorithm enables the UAVs to maximize area coverage within a given number of time-steps, and the second algorithm enables the UAVs to achieve a desired coverage level while minimizing the required number of movements. The focus of this work is on ensuring continuous multi-hop connectivity of the UAVs with the base station using inter-UAV communication links. Based on extensive performance analysis, we conclude that factors such as the base station location, connectivity requirements, and number of UAVs can have a significant impact on the performance of the proposed algorithms. These aspects should be carefully considered in the design of such UAV-based surveillance networks.

While the proposed methods rely on offline path computation in a static environment, practical deployments often involve dynamic and unpredictable conditions. To address potential disruptions due to sudden battery drain, environmental changes, obstacles, or node failures, our future work will focus on incorporating real-time adaptability into the system. In particular, we plan to explore online and learning-based strategies, such as reinforcement learning or distributed decision-making, to enable responsive and resilient UAV path planning.

CRediT authorship contribution statement

Survi Kumari: Writing – original draft, Formal analysis, Methodology. **Seshan Srirangarajan:** Writing – review & editing, Supervision, Project administration, Funding acquisition, Conceptualization.

Declaration of competing interest

The authors declare that they have no known competing financial interests or personal relationships that could have appeared to influence the work reported in this paper.

Data availability

No data was used for the research described in the article.

References

[1] C. Zygowski, A. Jaekel, Optimal path planning strategies for monitoring coverage holes in wireless sensor networks, Ad Hoc Netw. 96 (2020) 101990, http://dx.doi.org/10.1016/j.adhoc.2019.101990.

[2] A.V. Savkin, H. Huang, A method for optimized deployment of a network of surveillance aerial drones, IEEE Syst. J. 13 (4) (2019) 4474–4477, http://dx.doi.org/10.1109/JSYST.2019.2910080.

[3] H. Niu, N. Gonzalez-Prelcic, R.W. Heath, A UAV-based traffic monitoring system - invited paper, in: IEEE Veh. Technol. Conf., 2018, pp. 1–5, http://dx.doi.org/10.1109/VTCSpring.2018.8417546.

[4] G. Danoy, M.R. Brust, P. Bouvry, Connectivity stability in autonomous multi-level UAV swarms for wide area monitoring, in: ACM Symp. Dev. Anal. Intell. Veh. Netw. Appl., 2015, pp. 1–8, http://dx.doi.org/10.1145/2815347.2815351.

[5] M.-A. Messous, S.-M. Senouci, H. Sedjelmaci, Network connectivity and area coverage for UAV fleet mobility model with energy constraint, in: IEEE Wirel. Commun. Netw. Conf., 2016, pp. 1–6, http://dx.doi.org/10.1109/WCNC.2016.7565125.

[6] E. Yanmaz, Connectivity versus area coverage in unmanned aerial vehicle networks, in: IEEE Int. Conf. Commun., 2012, pp. 719–723, http://dx.doi.org/10.1109/ICC.2012.6364585.

[7] J.G. Jimenez, E. Moguel, J.G. Alonso, J. Berrocal, Energy-efficient and solar powered mission planning of UAV swarms to reduce the coverage gap in rural areas: The 3D case, Ad Hoc Netw. 118 (2021) 102517, http://dx.doi.org/10.1016/j.adhoc.2021.102517.

[8] S. Zhou, X. Liu, B. Tang, G. Tan, Handover and coverage analysis in 3-D mobile UAV cellular networks, IEEE Internet Things J. 11 (18) (2024) 29911–29925, http://dx.doi.org/10.1109/JIOT.2024.3407161.

[9] M. Rosalie, M.R. Brust, G. Danoy, S. Chaumette, P. Bouvry, Coverage optimization with connectivity preservation for UAV swarms applying chaotic dynamics, in: IEEE Int. Conf. Auton. Comput., 2017, pp. 113–118, http://dx.doi.org/10.1109/ICAC.2017.26.

[10] J. Li, Y. Xiong, J. She, M. Wu, A path planning method for sweep coverage with multiple UAVs, IEEE Internet Things J. 7 (9) (2020) 8967–8978, http://dx.doi.org/10.1109/JIOT.2020.2999083.

[11] C. Liu, H. Du, Q. Ye, Sweep coverage with return time constraint, in: IEEE Glob. Commun. Conf., 2016, pp. 1–6, http://dx.doi.org/10.1109/GLOCOM.2016.7842310.

[12] J. Chen, C. Du, Y. Zhang, P. Han, W. Wei, A clustering-based coverage path planning method for autonomous heterogeneous UAVs, IEEE Trans. Intell. Transp. Syst. 23 (12) (2022) 25546–25556, http://dx.doi.org/10.1109/TITS.2021.3066240.

[13] A. Lamine, F. Mguis, H. Snoussi, K. Ghedira, Linear models for total coverage problem with connectivity constraints using multiple unmanned aerial vehicles, Int. J. Sen. Netw. 34 (1) (2020) 15–25, http://dx.doi.org/10.1504/IJSNET.2020.109714.

[14] S. Kumari, S. Srirangarajan, Node placement and path planning for improved area coverage in mixed wireless sensor networks, IEEE Robot. Autom. Lett. 9 (8) (2024) 6800–6807, http://dx.doi.org/10.1109/LRA.2024.3412590.

[15] A. Chapnevis, E. Bulut, UAV mesh network trajectory planning for age optimal data collection in infrastructureless areas, in: IEEE Int. Conf. Commun., 2024, pp. 1563–1568, http://dx.doi.org/10.1109/ICC51166.2024.10622459.

[16] A. Chapnevis, E. Bulut, Delay optimal UAV trajectory planning for secure data collection from mobile IoT networks, in: IEEE Int. Conf. Ind. Technol., 2023, pp. 1–4, http://dx.doi.org/10.1109/ICIT58465.2023.10143110.

[17] A. Chapnevis, E. Bulut, AoI-optimal cellular-connected UAV trajectory planning for IoT data collection, in: IEEE Conf. Local Comput. Netw., 2023, pp. 1–6, http://dx.doi.org/10.1109/LCN58197.2023.10223376.

[18] A. Chapnevis, E. Bulut, Time-efficient approximate trajectory planning for AoI-centered multi-UAV IoT networks, IEEE Internet Things J. 29 (2025) 101461, http://dx.doi.org/10.1016/j.iot.2024.101461.

[19] H. Xie, D. Yang, L. Xiao, J. Lyu, Connectivity-aware 3D UAV path design with deep reinforcement learning, IEEE Trans. Veh. Technol. 70 (12) (2021) 13022–13034, http://dx.doi.org/10.1109/TVT.2021.3121747.

[20] Y. Gao, L. Xiao, F. Wu, D. Yang, Z. Sun, Cellular-connected UAV trajectory design with connectivity constraint: A deep reinforcement learning approach, IEEE Trans. Green Commun. Netw. 5 (3) (2021) 1369–1380, http://dx.doi.org/10.1109/TGCN.2021.3073916.

[21] Y.-J. Chen, D.-Y. Huang, Joint trajectory design and BS association for cellular-connected UAV: An imitation-augmented deep reinforcement learning approach, IEEE Internet Things J. 9 (4) (2022) 2843–2858, http://dx.doi.org/10.1109/JIOT.2021.3093116.

[22] X. Wang, M.C. Gursoy, Learning-based UAV trajectory optimization with collision avoidance and connectivity constraints, IEEE Trans. Wirel. Commun. 21 (6) (2022) 4350–4363, http://dx.doi.org/10.1109/TWC.2021.3129226.

[23] I. Guven, E. Yanmaz, Multi-objective path planning for multi-UAV connectivity and area coverage, Ad Hoc Netw. 160 (2024) 103520, http://dx.doi.org/10.1016/j.adhoc.2024.103520.